Science of the Total Environment 496 (2014) 75–83

Contents lists available at ScienceDirect

Science of the Total Environment

journal homepage: www.elsevier.com/locate/scitotenv

Dust episodes in Beirut and their effect on the chemical composition of coarse and fine particulate matter

Malek Jaafar [a], Rima Baalbaki [a], Raya Mrad [a,b], Nancy Daher [c], Alan Shihadeh [d], Constantinos Sioutas [c], Najat A. Saliba [a,*]

[a] American University of Beirut, Department of Chemistry, Beirut, Lebanon
[b] Unité de Chimie Environnementale et Interactions sur le Vivant (UCEIV), Université du Littoral-Côte d'Opale, France
[c] University of Southern California, Department of Civil and Environmental Engineering, Los Angeles, CA, USA
[d] American University of Beirut, Department of Mechanical Engineering, Beirut, Lebanon

HIGHLIGHTS

- An increase in particle volume for sizes between 2.25 and 5 μm
- Increase in crustal material in coarse and fine particles
- Biogenic enrichment of elements of anthropogenic origin like Ba and V
- Formation of organosulfates and organonitrates in fine PM

ARTICLE INFO

Article history:
Received 22 April 2014
Received in revised form 18 June 2014
Accepted 5 July 2014
Available online 26 July 2014

Editor: P. Kassomenos

Keywords:
Dust episodes
PM mass closure
Eastern Mediterranean city
Beirut
Organosulfates and organonitrates
Particle volume distribution

ABSTRACT

Particles captured during dust episodes in Beirut originated from both the African and Arabian deserts. This particular air mixture showed an increase, over non-dust episodes, in particle volume distribution which was mostly noticed for particles ranging in sizes between 2.25 and 5 μm. It also resulted in an increase in average mass concentration by 48.5% and 14.6%, for the coarse and fine fractions, respectively. Chemical analysis of major aerosol components accounted for 93% of fine PM and 71% of coarse PM. Crustal material (CM) dominated the coarse PM fraction, contributing to 39 ± 15% of the total mass. Sea salt (SS) (11 ± 10%) and secondary ions (SI) (11 ± 7%) were the second most abundant elements. In the fine fraction, SI (36 ± 14%) were the most abundant PM constituent, followed by organic matter (OM) (33 ± 7%) and CM (13 ± 2%). Enrichment factors (EF) and correlation coefficients show that biogenic and anthropogenic sources contribute to the elemental composition of particles during dust episodes. This study emphasizes on the role played by the long-range transport of aerosols in changing the chemical composition of the organic and inorganic constituents of urban coarse and fine PM. The chemical reactions between aged urban and dust aerosols are enhanced during transport, leading to the formation of organo-nitrogenated and -sulfonated compounds. Their oligomeric morphologies are further confirmed by SEM–EDX measurements.

1. Introduction

Dust episodes have been shown to affect particulate matter (PM) by increasing their mass loading to values above urban levels, and altering their chemical composition (i.e. (Bozlaker et al., 2013; Goudie and Middleton, 2001; Massoud et al., 2011; Rodríguez et al., 2001; Saliba et al., 2010; Saliba et al., 2007; Xie et al., 2005). Furthermore, dust has been known to be transported thousands of kilometers reaching places as far as Northern Europe (Franzén et al., 1994) and Amazonia (Swap et al., 1992). Even though dust storm episodes can vary in strength and duration (Gobbi et al., 2000), their remnants can remain in the atmosphere for a certain time after the storm ends (EU, 2011). This is also evident for African dust storms, where increases in PM_{10} levels remains up to one to three days after the dust episode ends ((EU, 2011) and references therein). Indeed African air mass intrusions develop vertically (Alpert et al., 2004; Balis et al., 2004; De Tomasi et al., 2003; Pérez, 2005) and considering the speed and size of particles, they will need around 2–3 days to deposit (Zender et al., 2003).

The Eastern Mediterranean region is one of the top dust storm generation regions in the world (Idso, 1976), with studies showing an increase in the number of dusty days (Alpert et al., 2004; Goudie and Middleton,

* Corresponding author. Tel.: +961 1 350000x3992; fax: +961 1 365217.
E-mail address: ns30@aub.edu.lb (N.A. Saliba).

http://dx.doi.org/10.1016/j.scitotenv.2014.07.018
0048-9697/

2001). Ganor et al. (2010) show that between 1958 and 2006, the number of dust episodes increased from 15 to 27, with a linear regression of 2.7 days per decade. This is of concern due to the association of morbidity with dust exposure, as documented by numerous epidemiological and biological studies (i.e. (Cheung et al., 2011; Perez et al., 2012; Tobías et al., 2011).

Despite this, the number of reported studies in this region is still scarce (i.e. (Dada et al., 2013; Daher et al., 2013; Ganor et al., 2010; Goudie and Middleton, 2006; Herut et al., 2001; Marconi et al., 2013; Massoud et al., 2011; Saliba et al., 2007), and an extrapolation from dust episode (of Saharan origin) studies in the Western Mediterranean would not be an accurate representation, mainly because the reported changes in PM composition remain specific to the local environmental and meteorological conditions (i.e. (Dayan et al., 1991; Ganor and Mamane, 1982; Griffin et al., 2007; Querol et al., 2009). This study focuses on the chemical and physical effect of dust episodes on urban PM in Beirut, a city that lies on the eastern coast of the Mediterranean Sea, surrounded by semi-arid regions and periodically subjected to dust storms originating from North Africa and the Arabian Peninsula. In this study, coarse ($PM_{10-2.5}$), particles with diameter between 2.5 and 10 μm, accumulation ($PM_{2.5-0.25}$), particles with diameter between 2.5 and 0.25 μm, and quasi-ultrafine ($PM_{0.25}$), particles with diameter less than 0.25 μm PM samples are collected during dust and non-dust episodes in Beirut. The four dust episodes identified in this study vary between dust and dust remnant. Gravimetric analysis and several analytical methods were used to determine the mass, particle distribution, the chemical composition, and the morphology during these particular episodes. It is also important to note that the results highlight the reaction of urban and long-range transport of dust aerosols to produce organo-sulfates and organo-nitrates.

2. Methods

2.1. Sample collection

Size-segregated PM samples were collected at the rooftop of the Chemistry department at the American University of Beirut (AUB), an urban background site located at 33°90′N, 35°50′E at an elevation of 20 m above ground level. From the south this site is surrounded by a green area with the nearest street located about 150 m away. From the north, it overlooks the Mediterranean Sea, separated by a two-lane road which is congested during morning and afternoon rush hours. From the Eastern side resides the Beirut harbor within a distance of 2.5 km. Particle levels at this site are commonly influenced by sea and land breeze circulation (Baalbaki et al., 2013).

The sampling campaign was conducted on dust and non-dust episodes during summer and fall of 2012. Dust episodes were identified based on forecasting air mass trajectories using daily forecast-trajectories calculated by the Hybrid Single Particle Lagrangian Integrated Trajectory Model (HYSPLIT) model (Draxler and Rolph, 2013) and relying on visual visibility limits and sky color. Those episodes were further confirmed using BSC-/DREAM dust maps (http://www.bsc.es/projects/earthscience/DREAM/) (Fig. S1). However, the residence time of transported dust particles is dependent upon the removal mechanisms, with residence times varying from few hours to 10 days (Goudie and Middleton, 2006; Kubilay et al., 2000; Papayannis et al., 2008). Moreover, if dust air masses are transported at high altitudes, they may affect ground level PM concentrations up to 2 days after an episode ends (EU, 2011). Therefore, in this study, dust episodes include days during which air mass trajectories were coming from the desert, and subsequent days where transported dust remnants possibly remain airborne. Moreover, the identity of these episodes was further confirmed using the Al data from the chemical analysis as a geo-chemical tracer. An average increase of 74% and 189% over non-dust episodes in the coarse and fine fractions, respectively, is reported. During the campaign, four dust episodes were identified, for which six samples were collected (Table S1, Fig. S1).

Coarse ($PM_{10-2.5}$), accumulation ($PM_{2.5-0.25}$) and quasi-ultrafine ($PM_{0.25}$) size-fractionated particles were collected using three parallel Sioutas Personal Cascade Impactor Samplers (Sioutas PCIS, SKC Inc., Eighty Four, PA, USA, (Misra et al., 2002)) preceded by PM_{10} inlets (Chemcomb Model 3500 Speciation Sampling Cartridge) and operating at a flow rate of 9 $L.min^{-1}$. Two PCISs were loaded with Teflon filters (Pall Life Sciences, Ann Arbor, MI) and were used for the analysis of: gravimetric mass, inorganic ions and total metals. The third PCIS was loaded with quartz filters (Whatman International Ltd.) and used for the analysis of water-soluble organic carbon (WSOC) as well as organic and elemental carbon (OC and EC, respectively).

Concurrently, 24 h PM samples were collected during dust episodes (November and December 2012) using a six stage cascade impactor (MPS — 6 Microanalysis Particle Sampler) of cut point sizes: 10, 5, 2.5, 1.0, 0.5 and 0.1 μm. Samples were collected either on 12 mm aluminum stubs coated with carbon adhesive tape or on ZnSe windows and used for SEM (Scanning Electron Microscope) imaging.

2.2. Sampling analysis

To determine PM mass concentration, prior to sectioning, Teflon filters were pre- and post-weighed using a UMX2 microbalance (Mettler Toledo GmbH, CH-8606 Greifensee, Switzerland), following 24 h equilibration under controlled temperature and relative humidity conditions (22–24 °C and 40–50%, respectively). The first set of Teflon filters was cut into 3 equal sections. The first section was analyzed for total elemental mass by means of a high resolution magnetic sector Inductively Coupled Plasma Mass Spectrometry (HR-ICP-MS Thermo-Finnigan Element 2). For the extraction, a microwave-aided Teflon bomb digestion protocol using a mixture of 1 mL of 16 M nitric acid, 0.25 mL of 12 M hydrochloric acid, and 0.10 mL of hydrofluoric acid was used (Herner et al., 2006). The digestion protocol was comprised of a 9 min ramp to 180 °C followed by a 10 min hold at 180 °C and 1 h of ventilation/cooling. Following cooling, digestates were diluted to 15 mL with high purity water then analyzed by HR-ICP-MS (Lough et al., 2005). The second section was extracted with high purity water and used to quantify PM concentrations of water-soluble inorganic ions using ion chromatography (Model 2020i, Dionex Corp.) The third section and second set of Teflon filters were used for a separate study.

Quartz filters, analyzed for Elemental Carbon, Organic Carbon and Water-Soluble Organic Carbon (EC, OC and WSOC, respectively), were prebaked at 550 °C for 12 h and stored in baked aluminum foil prior to sampling. Elemental and organic carbon contents of the filters were determined using the NIOSH Thermal Optical Transmission method (Birch and Cary, 1996). Water-soluble organic carbon content was quantified using a Sievers 900 Total Organic Carbon Analyzer, following water-extraction and filtration of the samples (Sullivan et al., 2004).

2.3. Chemical mass closure

For the purpose of chemical speciation, chemical components were classified into six categories: organic matter (OM), elemental carbon (EC), sea salt (SS), crustal material (CM), trace elements (TE) and secondary ions (SI). Organic matter was calculated by multiplying organic carbon (OC) by a factor of 2.1 in order to account for aged particles as recommended by several earlier studies (Gnauk et al., 2005; Sciare et al., 2005; Takahashi et al., 2008; Terzi et al., 2010). Sea salt was estimated as the sum of Na^+ concentration and sea-salt fractions of Cl^-, Mg^{2+}, K^+, Ca^{2+}, and SO_4^{2-} concentrations, assuming standard seawater composition (Seinfeld and Pandis, 2006). Crustal material includes typical crustal material elements (Al, K, Fe, Ca, Mg, Ti and Si) and was determined by summing the oxides of these metals using Eq. (1) with Ca and Mg representing their non-sea-salt fractions

(Chow et al., 1994; Hueglin et al., 2005; Marcazzan et al., 2001). Calcium was multiplied by a factor of 1.95 to account for both CaO and $CaCO_3$ (Remoundaki et al., 2013). Silicon, which was not measured in this study, was calculated by multiplying Al by a factor of 3.41 (Hueglin et al., 2005). Trace Elements containing other measured elements such as Cu, Zn, V, Mn, Cr, Sb… were determined by multiplying the concentrations of these elements by appropriate factors to convert them to their mineral oxides.

$$CM = 1.89Al + 1.4K + 1.43Fe + 1.95\,Ca + 1.66\,Mg + 1.67Ti + 2.14Si\,. \quad (1)$$

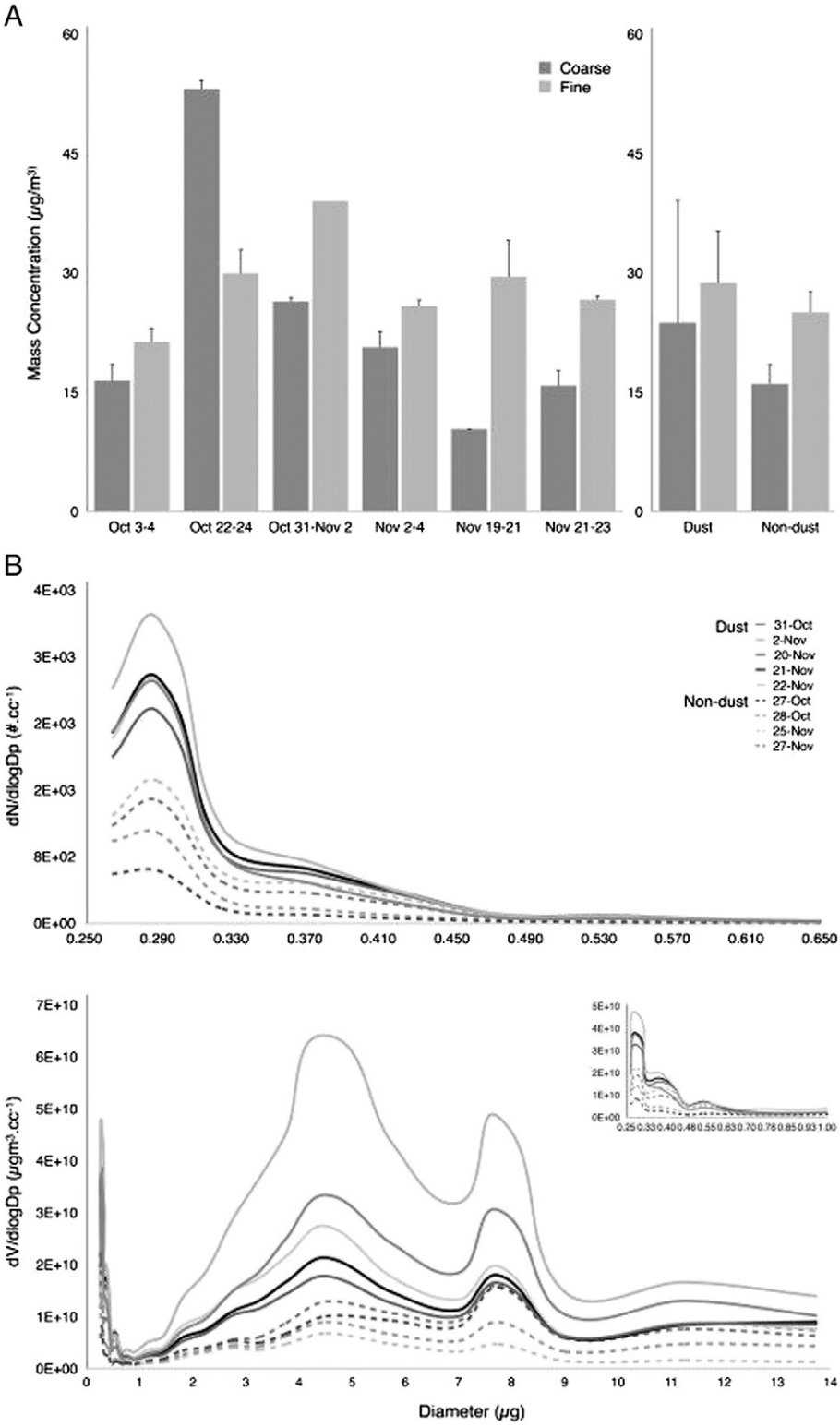

Fig. 1. Coarse and fine particle mass concentration (A) during dust episodes (upper left). Associated error bars represent the standard deviation of the gravimetric analysis of the two parallel Teflon filters. Average particle mass concentration during dust episodes compared to non-dust episodes (upper right). Number and volume size distribution (B) of particles with mean geometric diameter ranging between 0.265 and 15 µm during dust and non-dust episodes (bottom).

2.4. Particle size distribution

Particle number concentrations were measured using the Grimm EDM 365 system (GRIMM Aerosol Technik GmbH & Co. KG) deployed at the same site but at ground level. The system operates based on laser light scattering in 31 size channels ranging between 0.265 and 34 μm. Measurements are made every 6 s at a diode laser wavelength of 655 nm and particle count data were logged every 1 min.

2.5. Scanning electron microscope imaging

As described by Dada et al. (2013), the Scanning Electron Microscopy (SEM) (Tescan Model 51-XMX0010) operated along with an Energy Dispersive X-ray system (EDX) was used for elemental analysis. Voltage set at 20–30 KeV with 60 μA beam current allowed the detection of good quality images without damaging the sample. Several points on the same particle were analyzed by EDX in order to ensure homogeneity of particle composition. The spectra were then averaged.

Table 1
Coarse and fine PM composition during dust and non-dust episodes.

	Dust coarse	Dust fine	Non-dust coarse	Non-dust fine
OC (μg/m^3)	0.68 (0.20)	4.37 (0.78)	0.58 (0.05)	3.62 (1.24)
EC (μg/m^3)	0.06 (0.04)	1.95 (0.73)	0.03 (0.02)	1.76 (0.36)
Ions (μg/m^3)	3.29 (1.88)	11.75 (11.75)	3.62 (0.78)	16.34 (3.70)
Cl^-	0.52 (0.42)	0.03 (0.02)	0.46 (0.07)	0.02 (0.01)
NO_3^-	1.72 (0.92)	1.27 (1.03)	2.09 (0.78)	1.43 (0.97)
PO_4^-	0.00 (0.00)	0.08 (0.15)	0.00 (0.00)	0.00 (0.00)
SO_4^{2-}	0.39 (0.27)	5.72 (3.60)	0.35 (0.06)	9.73 (4.01)
Na^+	0.62 (0.44)	0.12 (0.10)	0.71 (0.28)	0.29 (0.31)
NH_4^+	0.00 (0.00)	4.37 (1.22)	0.00 (0.00)	4.73 (3.68)
K^+	0.05 (0.03)	0.16 (0.08)	0.02 (0.01)	0.14 (0.07)
Total metals (ng/m^3)	3387.81 (1373.88)	3269.50 (888.70)	3777.95 (1870.51)	3855.17 (1908.75)
Li	0.22 (0.10)	0.13 (0.06)	0.12 (0.09)	0.03 (0.02)
B	1.17 (4.00)	5.68 (2.62)	2.28 (2.13)	9.58 (4.81)
Na	640.89 (527.19)	142.90 (184.75)	932.58 (1087.26)	315.30 (156.17)
Mg	225.09 (101.87)	85.35 (35.87)	208.95 (166.68)	58.75 (39.87)
Al	365.60 (159.37)	190.37 (89.23)	209.76 (148.32)	65.79 (52.82)
P	8.59 (5.80)	16.51 (6.69)	2.30 (−)	8.47 (5.71)
S	154.20 (1165.23)	2022.08 (619.43)	110.25 (70.20)	2758.63 (1273.31)
K	119.62 (39.51)	167.50 (78.49)	89.90 (53.28)	161.16 (67.65)
Ca	1419.42 (711.00)	268.91 (104.47)	1084.25 (638.68)	257.37 (204.64)
Sc	0.09 (0.07)	0.05 (0.02)	0.05 (0.03)	0.23 (0.13)
Ti	31.55 (11.65)	16.12 (5.94)	18.51 (9.22)	8.54 (5.02)
V	2.27 (3.89)	16.20 (9.46)	0.79 (0.44)	10.85 (7.49)
Cr	1.12 (0.50)	0.31 (0.27)	0.57 (0.46)	0.03 (0.05)
Mn	5.40 (1.33)	4.66 (1.17)	3.11 (1.84)	4.03 (1.89)
Fe	374.52 (129.33)	215.37 (64.33)	199.85 (106.78)	121.90 (83.37)
Co	0.15 (0.07)	0.50 (0.39)	0.11 (0.08)	0.31 (0.25)
Ni	0.67 (1.68)	4.85 (3.13)	3.23 (4.57)	4.30 (3.16)
Cu	4.37 (4.78)	16.98 (15.93)	530.46 (1020.83)	14.96 (9.24)
Zn	14.06 (8.61)	60.44 (42.35)	312.34 (564.71)	31.98 (18.77)
As	0.09 (0.23)	0.38 (0.17)	0.11 (0.09)	0.60 (0.17)
Rb	0.50 (0.26)	0.41 (0.09)	0.24 (0.09)	0.55 (0.29)
Sr	3.83 (1.59)	1.56 (0.49)	2.84 (1.66)	1.21 (0.81)
Y	0.23 (0.21)	1.21 (1.00)	1.47 (1.82)	0.69 (0.51)
Nb	0.10 (0.03)	0.06 (0.02)	0.05 (0.03)	0.06 (0.01)
Mo	0.29 (0.26)	0.71 (0.32)	0.14 (0.09)	0.86 (0.62)
Rh	0.00 (0.00)	0.00 (0.00)	0.05 (0.09)	0.00 (0.00)
Pd	1.37 (1.02)	1.42 (0.45)	0.34 (0.34)	2.76 (1.82)
Ag	0.24 (0.24)	0.04 (0.04)	0.11 (0.10)	0.13 (0.06)
Cd	0.03 (0.08)	0.22 (0.12)	0.06 (0.09)	0.20 (0.12)
Sn	0.00 (0.16)	1.20 (1.52)	17.46 (−)	0.36 (0.19)
Sb	0.66 (0.18)	1.60 (1.01)	0.38 (0.30)	0.93 (0.52)
Cs	0.02 (0.01)	0.03 (0.01)	0.02 (0.01)	0.04 (0.02)
Ba	8.78 (2.66)	4.20 (1.56)	4.56 (2.50)	3.33 (2.73)
La	0.24 (0.08)	0.13 (0.06)	0.15 (0.09)	0.09 (0.07)
Ce	0.40 (0.15)	0.25 (0.09)	0.23 (0.12)	0.12 (0.01)
Pr	0.05 (0.02)	0.03 (0.01)	0.02 (0.01)	0.02 (0.02)
Nd	0.18 (0.07)	0.09 (0.03)	0.10 (0.05)	0.05 (0.04)
Sm	0.04 (0.01)	0.02 (0.01)	0.02 (0.01)	0.01 (0.00)
Eu	0.01 (0.00)	0.01 (0.00)	0.01 (0.00)	0.01 (0.00)
Dy	0.03 (0.01)	0.01 (0.01)	0.01 (0.01)	0.01 (0.00)
Ho	0.01 (0.00)	0.00 (0.00)	0.00 (0.00)	0.00 (0.00)
Yb	0.02 (0.01)	0.01 (0.00)	0.01 (0.00)	0.00 (0.00)
Lu	0.00 (0.00)	0.00 (0.00)	0.00 (0.00)	0.00 (0.00)
W	0.02 (0.02)	0.02 (0.01)	0.01 (0.01)	0.07 (0.03)
Pt	0.00 (0.02)	0.00 (0.00)	0.01 (0.00)	0.03 (0.01)
Tl	0.01 (0.02)	0.04 (0.03)	0.01 (0.01)	0.05 (0.02)
Pb	1.60 (4.08)	20.89 (11.98)	40.11 (70.08)	10.71 (4.58)
Th	0.05 (0.02)	0.03 (0.01)	0.03 (0.02)	0.08 (0.04)
U	0.03 (0.01)	0.01 (0.00)	0.02 (0.01)	0.01 (0.01)

3. Results and discussion

Coarse and fine (accumulation and quasi-ultrafine filters) size fractions were considered for the mass and chemical composition analysis of dust samples. The accumulation and quasi-ultrafine filters were composited together for the fine fraction due to the low PM mass collected, which would limit the number of chemical analyses that can be done.

Results were compared to those of non-dust episodes sampled during July and August 2012 (Daher et al., 2013). Because the fine fraction consisted of the sum of the accumulation and quasi-ultrafine filters, only the filters of non-dust episodes that were composited during analysis were considered.

3.1. Particle mass and size distribution

PM mass concentrations for the dust episodes ranged between 10 and 53 $\mu g \cdot m^{-3}$ for the coarse mode and between 21 and 39 $\mu g \cdot m^{-3}$ for the fine fraction. In comparison to the non-dust episodes, the coarse PM mass concentration increased by 48.5% while that of the fine increased by 14.6%, on average (Fig. 1-A). This is in agreement with other studies showing that desert dust intrusion has a larger effect on the increase of the mass concentration of the coarse PM (Lazaridis et al., 2008; Pérez et al., 2008).

Particle number and volume distributions for both dust and non-dust episodes are shown in Fig. 1-B. Similar particle number distribution patterns were observed during both dust and non-dust episodes. Nevertheless, particle number concentrations for dust episodes display an increase over non-dust episodes for all particle size bins averaging at a 146% increase in total particle counts. Similarly, particle volume distribution showed an increase ranging between 91 and 316% in all particle size bins between dust and non-dust episodes. This increase was most noticeable for particles ranging in sizes between 2.25 and 5 μm.

3.2. Chemical mass closure

The quantification of the different chemical components is summarized in Table 1 whereas the chemical mass reconstitution is shown in Fig. 2. In this study, almost full chemical mass closure was attained for fine PM of both dust and non-dust episodes, with the agreement between the reconstructed and gravimetric mass averaging 93% and 103%, respectively. On the other hand, identified coarse aerosol components accounted for 71 and 72% of the mass during dust and non-dust episodes, respectively. Unidentified PM mass is usually attributed to PM water content, where water is reported to constitute up to 35% of PM_{10} mass (Tsyro, 2005). Another possible explanation could be uncertainties associated with the factor used for the conversion of OC to OM. In fact, coarse PM contains high amounts of hygroscopic nitrates responsible for enhancing the hydrophilicity of coarse dust particles (Shi et al., 2008).

CM dominated the dust and non-dust coarse PM fractions with a 47% increase in CM contribution to PM during dust episodes (39 ± 15% and 26 ± 16% contribution to the total mass, respectively). Sea salt and secondary ions were the second most abundant elements. Sea salt accounted for 11 ± 10% of the dust coarse fraction and 15 ± 6% of the non-dust coarse fraction, while SI accounted for 11 ± 7% and 14 ± 4% of the dust and non-dust coarse fractions, respectively. The coarse PM composition of OM was similar during both dust (8 ± 1%) and non-dust (8 ± 1%) episodes. Notably, the difference between TE composition during dust and non-dust episodes was substantial, with a 1 ± 1% contribution in coarse dust versus 10 ± 18% in the non-dust samples. Finally, EC was the least abundant element in both dust and non-dust coarse samples, accounting for 0.3 ± 0.2 and 0.2 ± 0.1% of the mass, respectively.

In the fine PM fraction, SI contribution to the total mass was substantially higher during non-dust episodes (53 ± 14%) when compared to the dust episodes (36 ± 14%) calculating a 33% decrease in SI contribution to fine PM mass. Nevertheless, SI was the most abundant PM constituent during both episodes. The second most abundant species is OM, contributing to 33 ± 7% and 31 ± 12% of PM mass in the dust and non-dust fine mode, respectively. These results are in good agreement with other studies showing SI and OM as the main components of fine PM (Remoundaki et al., 2013). Crustal material constituted 13 ± 2% and 6 ± 4% of fine PM mass during dust and non-dust episodes, respectively, implying a 107% increase in CM contribution to fine PM mass during dust episodes. Elemental carbon had similar percentages during both episodes (7 ± 2%). TE constituted around 1% of the fine PM mass during both events, while SS constituted 5 and 4% of the dust and non-dust fine PM, respectively (Table 1). Overall, the six categories were assessed for their statistical significance. In comparison to non-dust data, all six categories were found to be statistically different with $p > 0.05$.

3.3. Enrichment factors and correlations

In order to assess the contribution of anthropogenic and natural sources to the PM chemical composition in both fractions, enrichment factors (EFs) for certain elements were calculated for the dust episodes. For each element, the EFs were estimated as the ratio of the abundance of the element in question with respect to Al to its average abundance in the upper continental crust with respect to Al as well (Fig. 3). The composition of the upper continental crust was obtained from Taylor and McLennan (1995). Usually, elements with EF close to 1 are considered of crustal origin, whereas those greater than 10 are of anthropogenic sources (Birmili et al., 2006; Chester et al., 1999; Pitts and Pitts, 2000;

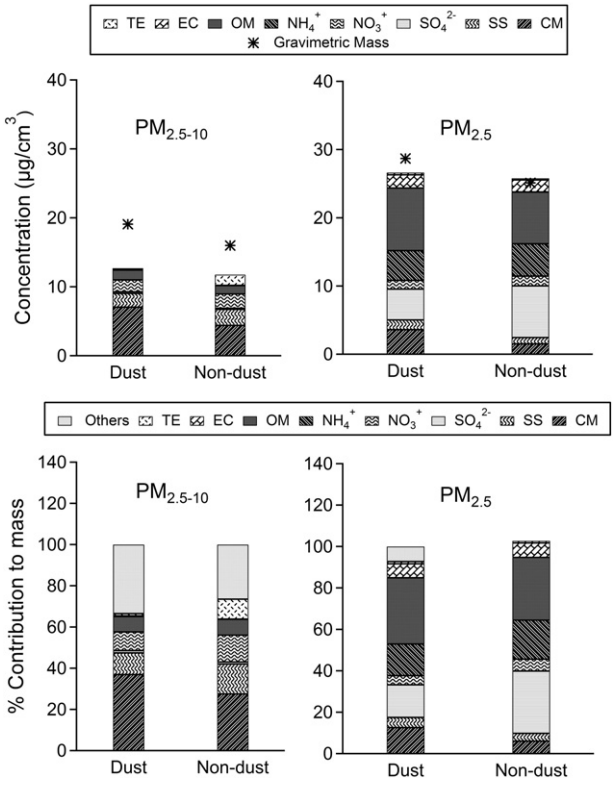

Fig. 2. Average chemical composition of coarse and fine PM in comparison to the total gravimetric mass represented by * (upper graph), and % contribution of the different chemical components to the total mass of coarse and fine PM (lower graph) during dust and non-dust events. Please note that Oct. 22–24 dust coarse PM filter was not included in the chemical analysis because it was overloaded.

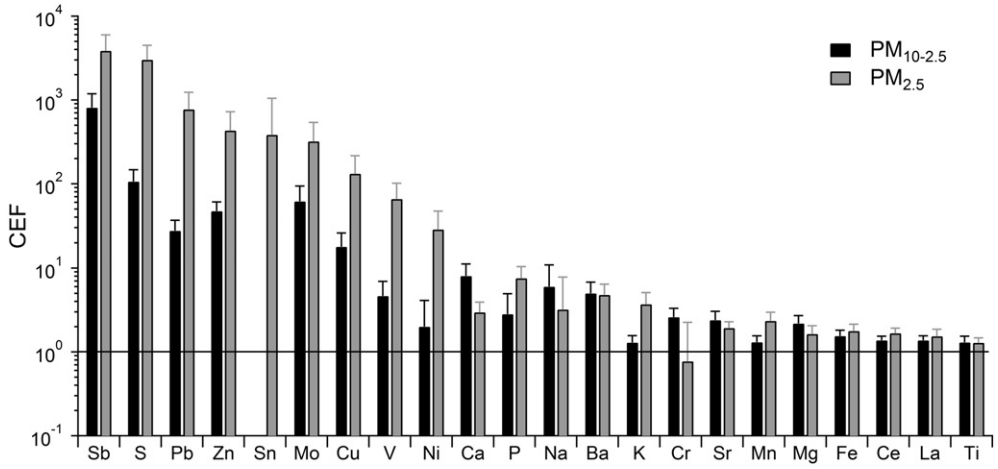

Fig. 3. Average enrichment factors in coarse and fine PM during dust episodes. Error bars represent standard deviation.

Torfs and Van Grieken, 1997). In addition, correlation between different components was calculated for better source apportionment (Table S2).

Elements like Ca, Cr, Sr, Mn, Mg, Fe, Ce, La and Ti display EFs close to 1 in both fractions, confirming their crustal origin, with Cr, Mn, Ce and La, being attributed to African dust (Finger and Helmy, 1998; Manoli et al., 2002; Remoundaki et al., 2013; Zhang et al., 2013). Although Ca had a relatively higher EF (EF ~10), it is considered to be of crustal origin due to its high correlation, in both fractions, with other crustal elements (Table S2). This high value is attributed to the abundance of calcite and limestone rocks in Lebanon (Abdel-Rahman and Nader, 2002; Kouyoumdjian and Saliba, 2006; Saliba et al., 2007), which is not well represented using the upper continental crustal composition values. Ba also showed EF close to 10, with high correlation with Sb ($r = 0.66$ and 0.77 in coarse and fine PM, respectively), which is a brake-wear tracer, suggesting that it is emitted mainly by anthropogenic sources (Daher et al., 2014; Sternbeck et al., 2002). However, it is also correlated with some crustal material (Cr, Fe, Ce, La) indicating that it also has some crustal origin (Engelbrecht et al., 2009). It is important to note that although Ba and Ca have similar EFs, their anti-correlation suggests that they do not originate from similar sources. Similarly, both Cu and Zn show EFs >10, and correlate with Sb, indicating their tire or brake wear origin (Lin et al., 2005). Ni and Mo, which were more enriched in the fine PM mode, are attributed to tracers of fuel and lube oil combustion, respectively (Isakson et al., 2001; Lu et al., 2006; Ntziachristos et al., 2007). Vanadium also shows a similar trend to Ni and Mo. Studies show that it might be derived from coal-powered plant emissions (Mamane et al., 1986; Ondov et al., 1989). Yet, its correlation with certain crustal elements, in the fine mode, suggests it is of biogenic sources as well (Dada et al., 2013; Engelbrecht et al., 2009).

3.4. Organosulfate and organonitrate in dust particles

Compared to dust episodes, the water-soluble nitrates and sulfates were more abundant in non-dust PM (Fig. 2). As shown in Table 2, high correlation coefficients of fine mode nitrates and sulfate ions with cations like Na^+, NH_4^+ and K^+ and elements like Mg and Ca during non-dust episodes indicate a strong association between these elements. Furthermore, higher soluble fractions of sulfur during non-dust episodes reflected by the Sulfate/Sulfur ratios (SO_4/total S = 2.5 in dust and 3.1 in non-dust coarse PM samples, and 2.8 and 3.5 in dust and non-dust fine PM samples, respectively) confirm the association of sulfates with soluble cations in particles.

However, during dust episodes, SEM–EDX analysis indicated the presence of oligomers of organo-sulfates and organo-nitrates as shown in Fig. 4. Fig. 4D was used as a reference to show particles of the same size during non-dust events. The morphology and EDX analysis indicated the presence of nitrogen, sulfur and oxygen, as principle components in the accumulation mode (0.5–0.1 μm) of particles collected on carbon tapes during dust episodes of November 2012 (Fig. 4, A–C). However, when the carbon contribution to the elemental composition of the observed structures could not be determined due to carbon interferences from the substrate; sampling on ZnSe windows was adopted during the dusty episode of December 29, 2012 (Fig. 4, E–I). Similar composition and morphology suggest that organosulfates and organonitrates form oligomeric patterns in aerosols. The fact that these species are larger than the impactor cut-off diameter is explained by Denkenberger et al. (2007), where a higher degree of oligomerization is detected in smaller particle mode (140–200 nm). Additionally, it is reported that oligomeric species exhibit an increase in the particle mass

Table 2
Spearman correlation coefficients (R) between fine nitrates, sulfates and sulfur and selected species during dust and non-dusty episodes. Values in Parentheses represent the p-value. R values higher than 0.50 are bolded.

PM components	Non-dusty						
	Na^+	NH_4^+	K^+	Mg	Ca	OM	WSOM
NO_3^-	0.87 (0.32)	0.16 (0.95)	0.37 (0.31)	0.90 (0.31)	0.95 (0.32)	0.53 (0.55)	0.98 (0.80)
SO_4^{2-}	**0.99 (0.05)**	**0.63 (0.18)**	**0.77 (0.05)**	**0.99 (0.05)**	**0.97 (0.05)**	0.05 (0.07)	0.77 (0.29)
S	0.97 (0.03)	0.77 (0.23)	0.89 (0.02)	0.96 (0.02)	0.91 (0.02)	−0.16 (0.30)	0.62 (0.06)
PM components	Dusty						
	Na^+	NH_4^+	K^+	Mg	Ca	OM	WSOM
NO_3^-	0.08 (0.04)	0.46 (0.00)	0.16 (0.04)	−0.23 (0.04)	0.10 (0.06)	**0.74 (0.00)**	**0.80 (0.00)**
SO_4^{2-}	0.17 (0.01)	0.36 (0.42)	−0.33 (0.01)	−0.21 (0.01)	0.16 (0.01)	0.33 (0.07)	0.32 (0.96)
S	0.09 (0.00)	0.60 (0.02)	0.26 (0.00)	0.13 (0.00)	0.22 (0.00)	**0.79 (0.00)**	**0.60 (0.00)**

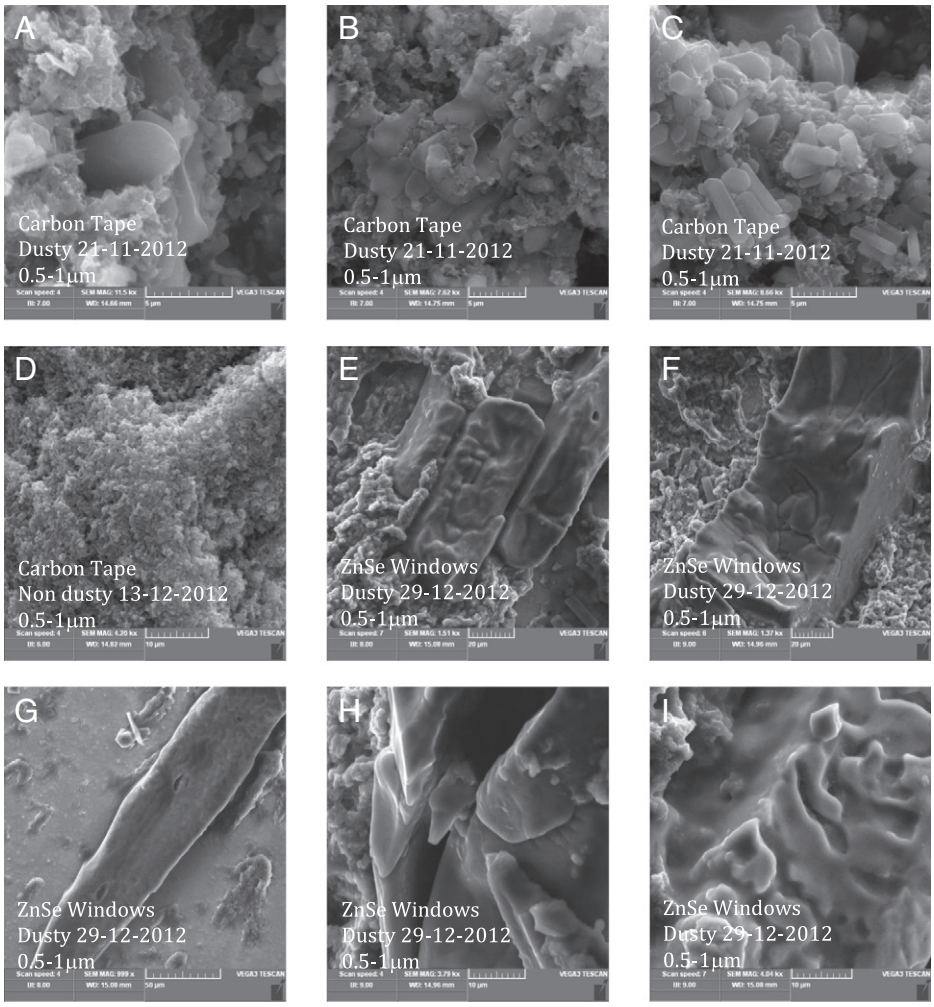

Spectrum	C	N	O	Al	Si	S	K	Ca
A	51.8		38.6	0.2	0.7	8.7		
B	40.5	15.3	36.6	0.5	1.0	5.6	0.2	0.3
C	33.9		49		0.2	16.9		
D	61.1	10.5	25.8			2.2	0.2	
E	16.5	18.5	50.7			14.1	0.2	
F	10.7	14.9	57.1			17.1	0.2	
G	4.7	24.7	58.4			11.8	0.4	
H	34.1	18.9	41.5			5.3	0.2	
I	19.6	13.2	50.9			16.1	0.2	

Fig. 4. SEM images and EDX atomic percentages for fine particulate matter on carbon tape and ZnSe windows sampled on November and December 2012.

spectral intensity and constitute an important component of secondary organic aerosol (SOA) mass that can reach up to 80% of the total organic mass (Blando et al., 1998; Fuzzi et al., 2001; Romero and Oehme, 2005; Surratt et al., 2006). The presence of these organo-sulfates and organo-nitrates was further confirmed by the correlation of nitrates and total sulfur with organic matter (OM and WSOM) in fine particles (Table 2).

In brief, it is deduced that the formation of urban organo-sulfates and organo-nitrates is enhanced in aged urban aerosols during dust episodes and their remnants.

4. Summary and conclusions

The physical and chemical characteristics of aerosols originating from a mixture of African and Arabian dust episodes in the Eastern Mediterranean region were investigated in the city of Beirut. Results of this study show that dust episodes are accompanied with an overall increase in particle volume distribution in all particle size ranges but mostly noticed for particles ranging in sizes between 2.25 and 5 µm. This corresponds to an average increase in PM mass by approximately 1.5 and 1.2 times for the coarse and fine fractions, respectively. Because samples were collected during dust and remnant dust episodes, compared to non-dust episodes, the average contribution of crustal materials to PM mass was found to be 2.07 times higher in fine aerosols and only 1.34 times higher in coarse PM fractions. It is conceivable that remnant dust episodes may be rich in suspended aerosols mostly in the fine and ultrafine sizes. The elemental analysis clearly showed the contribution of anthropogenic (Cu, Zn, Sb, Mo, Ni) and biogenic (Ca, Cr, Sr, Mn, Mg, Mn, Fe, Ce, La, Ti) sources during both dust and

non-dust episodes, with elements, like Ba and V, being influenced by both. Enrichment of fine and ultrafine particles with organo-nitrogenated and sulfonated compounds was particularly pronounced during dust episodes. These chemical components are the result of chemical transformations of dust with urban aerosols originating from local and long-range transport.

Acknowledgements

This work has been supported by the Lebanese National Council for Scientific Research (CNRS #21444) and by the American University Research Board (URB) at AUB (URB #21058). The authors gratefully acknowledge the NOAA Air Resources Laboratory (ARL) for the provision of the HYSPLIT transport and dispersion model and/or READY website (http://ready.arl.noaa.gov) used in this publication. The authors gratefully acknowledge the Central Research Science Laboratory team for their help in the SEM optimization. The authors also would like to thank USC Provost's Ph.D. fellowship and the staff at Wisconsin State Laboratory of Hygiene for their assistance with the chemical measurements.

Appendix A. Supplementary data

Supplementary data to this article can be found online at http://dx.doi.org/10.1016/j.scitotenv.2014.07.018.

References

Abdel-Rahman AF, Nader FH. Characterization of the Lebanese Jurassic–Cretaceous carbonate stratigraphic sequence: a geochemical approach. Geol J 2002;37:69–91.
Alpert P, Kishcha P, Shtivelman A, Krichak SO, Joseph JH. Vertical distribution of Saharan dust based on 2.5-year model predictions. Atmos Res 2004;70:109–30.
Baalbaki R, Al-Assaad K, Mehanna CJ, Saliba NA, Katurji M, Roumié M. Road versus roadside particle size distribution in a hot Mediterranean summer—estimation of fleet emission factors. J Air Waste Manag Assoc 2013;63:327–35.
Balis DS, Amiridis V, Nickovic S, Papayannis A, Zerefos C. Optical properties of Saharan dust layers as detected by a Raman lidar at Thessaloniki, Greece. Geophys Res Lett 2004;31.
Birch ME, Cary RA. Elemental carbon-based method for occupational monitoring of particulate diesel exhaust: methodology and exposure issues. Analyst 1996;121:1183–90.
Birmili W, Allen AG, Bary F, Harrison RM. Trace metal concentrations and water solubility in size-fractionated atmospheric particles and influence of road traffic. Environ Sci Technol 2006;40:1144–53.
Blando JD, Porcja RJ, Li T-H, Bowman D, Lioy PJ, Turpin BJ. Secondary formation and the Smoky Mountain organic aerosol: an examination of aerosol polarity and functional group composition during SEAVS. Environ Sci Technol 1998;32:604–13.
Bozlaker A, Prospero JM, Fraser MP, Chellam S. Quantifying the contribution of long-range Saharan dust transport on particulate matter concentrations in Houston, Texas, using detailed elemental analysis. Environ Sci Technol 2013;47:10179–87.
Chester R, Nimmo M, Preston MR. The trace metal chemistry of atmospheric dry deposition samples collected at Cap Ferrat: a coastal site in the Western Mediterranean. Mar Chem 1999;68:15–30.
Cheung K, Daher N, Kam W, Shafer MM, Ning Z, Schauer JJ, et al. Spatial and temporal variation of chemical composition and mass closure of ambient coarse particulate matter (PM < sub > 10–2.5</sub>) in the Los Angeles area. Atmos Environ 2011;45:2651–62.
Chow JC, Watson JG, Fujita EM, Lu Z, Lawson DR, Ashbaugh LL. Temporal and spatial variations of PM2.5 and PM10 aerosol in the Southern California Air Quality Study. Atmos Environ 1994;28:2061–80.
Dada L, Mrad R, Siffert S, Saliba NA. Atmospheric markers of African and Arabian dust in an urban eastern Mediterranean environment, Beirut, Lebanon. J Aerosol Sci 2013;66:187–92.
Daher N, Saliba NA, Shihadeh AL, Jaafar M, Baalbaki R, Sioutas C. Chemical composition of size-resolved particulate matter at near-freeway and urban background sites in the Greater Beirut area. Atmos Environ 2013;80:96–106.
Daher N, Saliba NA, Shihadeh AL, Jaafar M, Baalbaki R, Shafer MM, et al. Oxidative potential and chemical speciation of size-resolved particulate matter (PM) at near-freeway and urban background sites in the Greater Beirut area. Sci Total Environ 2014;470–471:417–26.
Dayan U, Heffter J, Miller J, Gutman G. Dust intrusion events into the Mediterranean basin. J Appl Meteorol 1991;30:1185–99.
De Tomasi F, Blanco A, Perrone MR. Raman lidar monitoring of extinction and backscattering of African dust layers and dust characterization. Appl Optics 2003;42:1699–709.
Denkenberger KA, Moffet RC, Holecek JC, Rebotier TP, Prather KA. Real-time, single-particle measurements of oligomers in aged ambient aerosol particles. Environ Sci Technol 2007;41:5439–46.
Draxler RR, Rolph GD. HYSPLIT (HYbrid Single-Particle Lagrangian Integrated Trajectory) model access via NOAA ARL READY website [http://ready.arl.noaa.gov/HYSPLIT.php] Silver Spring, MD: NOAA Air Resources Laboratory; 2013.
Engelbrecht JP, McDonald EV, Gillies JA, Jayanty RKM, Casuccio G, Gertler AW. Characterizing mineral dusts and other aerosols from the Middle East—part 1: ambient sampling. Inhal Toxicol 2009;21:297–326.
EU. Commission staff working paper. Establishing Guidelines for Demonstration and Subtraction of Exceedances Attributable to Natural Sources under the Directive 2008/50/EC on Ambient Air Quality and Cleaner Air for Europe, Brussels, SEC (2011) 208 Final; 2011.
Finger E, Helmy HM. Composition and total-Pb model ages of monazite from high-grade paragneisses in the Abu Swayel area, southern Eastern Desert, Egypt. Mineral Petrol 1998;62:269–89.
Franzén LG, Hjelmroos M, Kållberg P, Brorström-Lunden E, Juntto S, Savolainen A-L. The 'yellow snowepisode'of northern Fennoscandia, March 1991—a case study of long-distance transport of soil, pollen and stable organic compounds. Atmos Environ 1994;28:3587–604.
Fuzzi S, Decesari S, Facchini MC, Matta E, Mircea M, Tagliavini E. A simplified model of the water soluble organic component of atmospheric aerosols. Geophys Res Lett 2001;28:4079–82.
Ganor E, Mamane Y. Transport of Saharan dust across the Eastern Mediterranean. Atmos Environ (1967) 1982;16:581–7.
Ganor E, Osetinsky I, Stupp A, Alpert P. Increasing trend of African dust, over 49 years, in the eastern Mediterranean. J Geophys Res 2010;115:D07201. http://dx.doi.org/10.1029/2009JD012500.
Gnauk T, Brüggemann E, Müller K, Chemnitzer R, Rüd C, Galgon D, et al. Aerosol characterisation at the FEBUKO upwind station Goldlauter (I): particle mass, main ionic components, OCEC, and mass closure. Atmos Environ 2005;39:4209–18.
Gobbi GP, Barnaba F, Giorgi R, Santacasa A. Altitude-resolved properties of a Saharan dust event over the Mediterranean. Atmos Environ 2000;34:5119–27.
Goudie AS, Middleton NJ. Saharan dust storms: nature and consequences. Earth Sci Rev 2001;56:179–204.
Goudie AS, Middleton NJ. Desert Dust in the Global System, vol. 2013. New York: Springer Berlin Heidelberg; 2006.
Griffin DW, Kubilay N, Koçak M, Gray MA, Borden TC, Shinn EA. Airborne desert dust and aeromicrobiology over the Turkish Mediterranean coastline. Atmos Environ 2007;41:4050–62.
Herner JD, Green PG, Kleeman MJ. Measuring the trace elemental composition of size-resolved airborne particles. Environ Sci Tech 2006;40:1925–33.
Herut B, Nimmo M, Medway A, Chester R, Krom MD. Dry atmospheric inputs of trace metals at the Mediterranean coast of Israel (SE Mediterranean): sources and fluxes. Atmos Environ 2001;35:803–13.
Hueglin C, Gehrig R, Baltensperger U, Gysel M, Monn C, Vonmont H. Chemical characterisation of PM2.5, PM10 and coarse particles at urban, near-city and rural sites in Switzerland. Atmos Environ 2005;39:637–51.
Idso SB. Dust storms. Sci Am 1976;235:108–15.
Isakson J, Persson TA, Selin Lindgren E. Identification and assessment of ship emissions and their effects in the harbour of Göteborg, Sweden. Atmos Environ 2001;35:3659–66.
Kouyoumdjian H, Saliba NA. Mass concentration and ion composition of coarse and fine particles in an urban area in Beirut: effect of calcium carbonate on the absorption of nitric and sulfuric acids and the depletion of chloride. Atmos Chem Phys 2006;6:1865–77.
Kubilay N, Nickovic S, Moulin C, Dulac F. An illustration of the transport and deposition of mineral dust onto the eastern Mediterranean. Atmos Environ 2000;34:1293–303.
Lazaridis M, Dzumbova L, Kopanakis I, Ondracek J, Glytsos T, Aleksandropoulou V, et al. PM10 and PM2.5 Levels in the Eastern Mediterranean (Akrotiri Research Station, Crete, Greece). Water Air Soil Pollut 2008;189:85–101.
Lin C-C, Chen S-J, Huang K-L, Hwang W-I, Chang-Chien G-P, Lin W-Y. Characteristics of metals in nano/ultrafine/fine/coarse particles collected beside a heavily trafficked road. Environ Sci Technol 2005;39:8113–22.
Lough GC, Schauer JJ, Park J-S, Shafer MM, DeMinter JT, Weinstein JP. Emissions of metals associated with motor vehicle roadways. Environ Sci Technol 2005;39:826–36.
Lu G, Brook JR, Rami Alfarra M, Anlauf K, Richard Leaitch W, Sharma S, et al. Identification and characterization of inland ship plumes over Vancouver, BC. Atmos Environ 2006;40:2767–82.
Mamane Y, Miller JL, Dzubay TG. Characterization of individual fly ash particles emitted from coal- and oil-fired power plants. Atmos Environ (1967) 1986;20:2125–35.
Manoli E, Voutsa D, Samara C. Chemical characterization and source identification/apportionment of fine and coarse air particles in Thessaloniki, Greece. Atmos Environ 2002;36:949–61.
Marcazzan GM, Vaccaro S, Valli G, Vecchi R. Characterisation of PM10 and PM2.5 particulate matter in the ambient air of Milan (Italy). Atmos Environ 2001;35:4639–50.
Marconi M, Sferlazzo DM, Becagli S, Bommarito C, Calzolai G, Chiari M, et al. Saharan dust aerosol over the central Mediterranean Sea: optical columnar measurements vs. aerosol load, chemical composition and marker solubility at ground level. Atmos Chem Phys Discuss 2013;13:21259–99.
Massoud R, Shihadeh A, Roumié M, Youness M, Gerard J, Saliba N, et al. Intraurban variability of PM10 and PM2.5 in an Eastern Mediterranean city. Atmos Res 2011;101:893–901.
Misra C, Singh M, Shen S, Sioutas C, Hall PM. Development and evaluation of a personal cascade impactor sampler (PCIS). J Aerosol Sci 2002;33:1027–47.
Ntziachristos L, Ning Z, Geller MD, Sheesley RJ, Schauer JJ, Sioutas C. Fine, ultrafine and nanoparticle trace element compositions near a major freeway with a high heavy-duty diesel fraction. Atmos Environ 2007;41:5684–96.

Ondov JM, Choquette CE, Zoller WH, Gordon GE, Biermann AH, Heft RE. Atmospheric behavior of trace elements on particles emitted from a coal-fired power plant. Atmos Environ (1967) 1989;23:2193–204.
Papayannis A, Amiridis V, Mona L, Tsaknakis G, Balis D, Bösenberg J, et al. Systematic lidar observations of Saharan dust over Europe in the frame of EARLINET (2000–2002). J Geophys Res Atmos 2008;113:D10204.
Pérez C. Local to regional atmospheric modeling and aerosol lidar methods in the Mediterranean [Tesis Doctoral Universidad Politécnica de Cataluña]; 2005.
Pérez N, Pey J, Castillo S, Viana M, Alastuey A, Querol X. Interpretation of the variability of levels of regional background aerosols in the Western Mediterranean. Sci Total Environ 2008;407:527–40.
Perez L, Tobías A, Querol X, Pey J, Alastuey A, Díaz J, et al. Saharan dust, particulate matter and cause-specific mortality: a case–crossover study in Barcelona (Spain). Environ Int 2012;48:150–5.
Pitts BJF, Pitts JN. Chemistry of the upper and lower atmosphere: theory, experiments and applications. New York: Academic Press; 2000.
Querol X, Pey J, Pandolfi M, Alastuey A, Cusack M, Pérez N, et al. African dust contributions to mean ambient PM < sub > 10</sub > mass-levels across the Mediterranean Basin. Atmos Environ 2009;43:4266–77.
Remoundaki E, Kassomenos P, Mantas E, Mihalopoulos N, Tsezos M. Composition and mass closure of $PM_{2.5}$ in urban environment (Athens, Greece). Aerosol Air Qual Res 2013;13:72–82.
Rodŕıguez S, Querol X, Alastuey A, Kallos G, Kakaliagou O. Saharan dust contributions to PM10 and TSP levels in Southern and Eastern Spain. Atmos Environ 2001;35:2433–47.
Romero F, Oehme M. Organosulfates—a new component of humic-like substances in atmospheric aerosols? J Atmos Chem 2005;52:283–94.
Saliba NA, Kouyoumdjian H, Roumié M. Effect of local and long-range transport emissions on the elemental composition of p M10–2.5 and PM2.5 in Beirut. Atmos Environ 2007;41:6497–509.
Saliba NA, El Jam F, El Tayar G, Obeid W, Roumie M. Origin and variability of particulate matter (PM10 and PM2.5) mass concentrations over an Eastern Mediterranean city. Atmos Res 2010;97:106–14.
Sciare J, Oikonomou K, Cachier H, Mihalopoulos N, Andreae MO, Maenhaut W, et al. Aerosol mass closure and reconstruction of the light scattering coefficient over the Eastern Mediterranean Sea during the MINOS campaign. Atmos Chem Phys 2005;5:2253–65.
Seinfeld JH, Pandis SN. Atmospheric chemistry and physics: from air pollution to climate change. 2nd ed. New Jersey: John Wiley and Sons; 2006.
Shi Z, Zhang D, Hayashi M, Ogata H, Ji H, Fujiie W. Influences of sulfate and nitrate on the hygroscopic behaviour of coarse dust particles. Atmos Environ 2008;42:822–7.
Sternbeck J, Sjödin Å, Andréasson K. Metal emissions from road traffic and the influence of resuspension—results from two tunnel studies. Atmos Environ 2002;36:4735–44.
Sullivan AP, Weber RJ, Clements AL, Turner JR, Bae MS, Schauer JJ. A method for on-line measurement of water-soluble organic carbon in ambient aerosol particles: results from an urban site. Geophys Res Lett 2004;31:L13105. [1–4].
Surratt JD, Murphy SM, Kroll JH, Ng NL, Hildebrandt L, Sorooshian A, et al. Chemical composition of secondary organic aerosol formed from the photooxidation of isoprene. J Phys Chem A 2006;110:9665–90.
Swap R, Garstang M, Greco S, Talbot R, Kållberg P. Saharan dust in the Amazon Basin. Tellus B 1992;44:133–49.
Takahashi K, Minoura H, Sakamoto K. Chemical composition of atmospheric aerosols in the general environment and around a trunk road in the Tokyo metropolitan area. Atmos Environ 2008;42:113–25.
Taylor SR, McLennan SM. The geochemical evolution of the continental crust. Rev Geophys 1995;33:241–65.
Terzi E, Argyropoulos G, Bougatioti A, Mihalopoulos N, Nikolaou K, Samara C. Chemical composition and mass closure of ambient PM10 at urban sites. Atmos Environ 2010;44:2231–9.
Tobías A, Caylà JA, Pey J, Alastuey A, Querol X. Are Saharan dust intrusions increasing the risk of meningococcal meningitis? Int J Infect Dis 2011;15:e503.
Torfs K, Van Grieken R. Chemical relations between atmospheric aerosols, deposition and stone decay layers on historic buildings at the Mediterranean coast. Atmos Environ 1997;31:2179–92.
Tsyro SG. To what extent can aerosol water explain the discrepancy between model calculated and gravimetric PM10 and PM2.5? Atmos Chem Phys 2005;5:515–32.
Xie S, Yu T, Zhang Y, Zeng L, Qi L, Tang X. Characteristics of PM₁₀SO<sub>2-/sub>NO_x and O₃ in ambient air during the dust storm period in Beijing. Sci Total Environ 2005;345:153–64.
Zender CS, Bian H, Newman D. Mineral Dust Entrainment and Deposition (DEAD) model: description and 1990s dust climatology. J Geophys Res Atmos (1984–2012) 2003;108.
Zhang R, Jing J, Tao J, Hsu S-C, Wang G, Cao J, et al. Chemical characterization and source apportionment of $PM_{2.5}$ in Beijing: seasonal perspective. Atmos Chem Phys 2013;13:7053–74.